Probabilistic Engineering Mechanics 83 (2026) 103903

Contents lists available at ScienceDirect

Probabilistic Engineering Mechanics

journal homepage: www.elsevier.com/locate/probengmech

Refining the masonry shear modulus in masonry towers via Bayesian model updating

Silvia Monchetti [a,*], Gianni Bartoli [a], Michele Betti [a], Siro Casolo [b], Francesco Clementi [c]

[a] Department of Civil and Environmental Engineering, University of Florence, via di S. Marta 3 – I, 50139, Florence, Italy
[b] Department ABC, Politecnico di Milano, Piazza Leonardo da Vinci 32, 20133, Milano, Italy
[c] Department of Civil and Building Engineering and Architecture, Polytechnic University of Marche, via Brecce Bianche, 60131, Ancona, Italy

ARTICLE INFO

Keywords:
Bayesian inference
Model updating
Rigid body-spring model (RBSM)
Historic masonry towers
Experimental data
Shear modulus

ABSTRACT

The assessment of the structural behavior of masonry towers often involves developing and identifying computational models to be used to perform static and/or time-history nonlinear analyses. Such models are frequently developed assuming isotropic masonry behavior, with model identification carried out - based on available experimental data - through deterministic tuning of a limited set of representative parameters. However, masonry exhibits complex structural textures that often deviate significantly from the commonly made assumption of isotropic behaviour. This paper investigates the effects of this assumption by focusing on the masonry shear modulus. A two-dimensional rigid body–spring model is adopted as computational approach, as its fully discrete formulation allows overcoming the limitations of the Cauchy continuum while maintaining a reduced computational cost. A Bayesian updating framework based on dynamic experimental data is employed to account for multiple sources of uncertainty, including parameter uncertainty, model inadequacy, and observation errors. Three masonry towers with different slenderness ratios are considered as representative case studies. The adopted Bayesian model updating approach allows for the estimation of their shear modulus while accounting for uncertainties, and the results show that the common assumption of isotropic behaviour in masonry numerical modelling does not hold. Using a fully discrete computational approach in combination with experimental frequency data, this behaviour has been observed for squat masonry towers.

1. Introduction

The definition of a reliable computational model of a structure based on the achieved level of knowledge (in terms of geometry, material properties, restraint conditions, etc.) is the first step when investigating the structural response of a historical building. It is within this framework that the heterogeneity of the historic masonries and the difficulties in performing exhaustive experimental tests may act as a hindrance to the proper identification of the masonry mechanical properties thus negatively affecting the reliability of the computational model (Cattari et al. [1]).

Masonry material is characterized by an inelastic, anisotropic, non-symmetric and non-homogeneous behaviour, and includes a huge variety of typologies which differ in terms of components and texture. All this makes it difficult to estimate the mechanical properties of a specific masonry arrangement simply starting from the characteristics of its components (also because they depend on many other parameters such as the integrity of the walls and the stress level that has been experienced). The modelling of the current masonry behaviour is so challenging that some assumptions and simplifications are required, often taken for granted *e.g.* the hypothesis of isotropic elasticity. This approach complies with the current code procedure for the determination of the mechanical properties of existing masonry in terms of compressive and shear strength, Young's modulus and shear modulus (see *e.g.* NTC [2]).

However, as underlined by Cattari and Magenes [3], an inconsistency arises from the anisotropic and heterogeneous nature of masonry, because the ratio between Young's modulus and shear modulus gathered from experimental tests or literature studies often leads to values that seem unrealistic when interpreted within the framework of an elastic,

* Corresponding author.
E-mail addresses: silvia.monchetti@unifi.it (S. Monchetti), gianni.bartoli@unifi.it (G. Bartoli), michele.betti@unifi.it (M. Betti), siro.casolo@polimi.it (S. Casolo), francesco.clementi@univpm.it (F. Clementi).

https://doi.org/10.1016/j.probengmech.2026.103903
Received 24 October 2025; Received in revised form 2 February 2026; Accepted 12 February 2026
Available online 13 February 2026

homogeneous, isotropic material. It is well known that experimental results from flat-jack, diagonal compression, uniaxial compression, and shear–compression tests reported in the scientific literature exhibit a large scatter in these parameters (Tomaževič [4], Boschi et al. [5], Casolo et al [6], Betti and Galano [7]). These aspects raise the question of how the modelling strategies can handle the peculiar behaviour of historical masonry. Indeed, different assumptions can be used for representing the constitutive laws (see *e.g.* D'Altri et al. [8], Schiavoni et al. [9]) and different approaches can be adopted to take into account the uncertainties on the mechanical properties of the masonry (see *e.g.* Monchetti et al. [10]).

Among the different mechanical properties of the masonry, the definition of the actual elastic shear modulus is particularly demanding due to the invasiveness of the experimental tests required for its direct evaluation (Corradi et al. [11], Brignola et al. [12], Andreini et al. [13], Borri et al. [14]). In this context, Bosiljkov et al. [15] and Tomaževič [4] critically analysed the shear modulus values proposed by Eurocode 6 CEN ([16]), which appear excessively high when compared with experimental evidence. Because of the inelastic, non-homogeneous, non-symmetric and anisotropic nature of masonry, the ratio between shear modulus and Young's modulus has been shown to vary widely, typically within the range of 6–25% according to experimental evidence. Values that are nowhere near those provided by Eurocode 6 (CEN [16]) (40%). More recently, Croce et al. [17] gathered a large database on masonry shear properties, highlighting a substantial scatter in shear modulus values resulting from different experimental test arrangements. According to the average values resulting from experiments, Croce et al. [17] suggested to define the shear modulus as approximately 15% of the Young's modulus.

From the numerical modeling perspective, it is therefore necessary to describe the response of the masonry system by explicitly accounting for the effects of the significant scatter observed in its mechanical parameters through appropriate computational models. On the one hand, these models should be simple enough to allow extensive parametric analyses; on the other hand, they should be capable to account for the peculiar behaviour of masonry material. To address both requirements, a Rigid Body-Spring Model (RBSM) has been proposed in literature as a computational method able to combine these two requirements (Casolo [18]). From an engineering point of view, the heterogeneous solid material is represented as a "mechanism" made by the assembly of rigid elements connected by elastic springs within the Rigid Body–Spring Model framework, originally developed by Kawai [19]. This result in a full discrete approach, which has already been employed and extensively tested in the scientific literature for the numerical analysis of masonry towers (Casolo et al. [20]) and has proven efficient in dealing with dynamic and nonlinear analyses. It has also been adopted to investigate the need for specific orthotropic damage modelling in the in-plane shear behavior of ancient masonry towers (Casolo [21]) by showing that this approach leads to reliable results. Being the RBSM a fully discrete approach it results particularly useful for the scope of this study, as it allows for the straightforward implementation and management of the masonry anisotropic mechanical behaviour. Recently, D'Altri et al. [22] reported the growing interest in alternative modeling strategies by calibrating different constitutive models for masonry panels, including discrete macro-element approaches in which the shear modulus is treated independently of Young's modulus.

In this context, this study focuses on the updating of the masonry shear parameter considering the structural typology of masonry towers by combining RBSM anisotropic modelling with Bayesian inference based on dynamic experimental data. The proposed approach, applied to slender and squat masonry towers, allows the estimation of the shear modulus accounting for uncertainty and rigorously specifies the key role of the masonry shear modulus in model identification. Comparison with conventional isotropic computational models shows that matching experimental observations requires shear parameters that do not comply with the commonly assumed isotropic behaviour, as supported by experimental studies. The proposed framework, which combines anisotropic modelling with Bayesian inference based on experimental frequency data, allows this result to be verified for squat masonry towers.

To discuss these issues, the paper is organized as follows. Section 2 reports the research aim while Section 3 introduces the methodology. Section 4 presents the case study. Section 5 illustrates the Bayesian model updating though the result discussion and, eventually, Section 6 reports the lessons learned.

2. Research aim

Historic masonry towers represent the object of the present research, which rises to the challenge to provide useful tools and reliable methods to ensure the optimal use of the resources required for the tasks of control, preservation, and repair. With this aim, three isolated masonry towers were used as reference cases. The towers exhibit different slenderness, *i.e.* different ratios between the total height and the length of the outer side of the base cross-section. This parameter may be useful for investigating their different effects of the shear deformability on the dynamic response. The geometry of the towers is deduced from existing available documentation (cross-section, front and planar views). Moreover, these towers have been the object of previous studies which were focused on the calibration of the Young's Modulus by reducing the discrepancy between the numerical model output and the experimental observations in terms of natural frequencies and modal shapes; see *e.g.* the works of Lacanna et al. [23], Standoli et al. [24], and Milani and Clementi [25], Ferrante et al. [26]. Within this background, the present paper proposes an Uncertainty Quantification (UQ) point of view of these three towers to infer, via Bayes' theorem, the shear modulus of the masonry with the observation of the natural frequencies by using a specific rigid body-spring model. The aim is to investigate if the observation of the natural frequencies can be used to infer the ratio between the Young's modulus and the shear modulus of the masonry. For this purpose, the well-known relationship which links Young's modulus, Poisson's coefficient and shear modulus in an isotropic continuum, $G = E/[2(1+\nu)]$, is not assumed a priori.

3. Materials and methods

This section summarizes the methodology used in this research by describing the two main steps: (i) the numerical model definition and (ii) the probabilistic characterization of the system. For evaluating the effect of the masonry shear modulus in the calibration of the model for historic towers, this paper takes advantage of the observed data from Ambient Vibration Testing and develops a numerical model to reproduce the dynamic behaviour of the system by using the RBSM in a Bayesian inference framework.

3.1. Rigid body and spring model (RBSM)

The numerical simulation of the dynamic behaviour of the masonry structure is herein carried out by using RBSM. The aim is to apply this modelling technique in the field of linear dynamical analysis, to identify the main modal features of a masonry structure.

Some RBSM applications on historical masonry structures are available in literature (see *e.g.* Casolo et al. [20], Bertolesi et al. [27]), where the RBSM demonstrates its effectiveness in reproducing (adopting proper constitutive relations) the in-plane and out of plane behaviour of façades and towers. A fully discrete approach is chosen to implement the numerical model adopted to evaluate the dynamical response of the tower. The masonry material is discretized at the macro-scale by a specific assemblage of rigid elements connected by elastic-plastic spring-bonds. The basic concept of this approach is that the main macroscopic mechanical parameters of the heterogeneous material can be resumed by a heuristic-molecule (Casolo [28], Casolo [21])

composed of 4 rigid masses connected by line-springs, as shown in Fig. 1, arranged according to a topology which is apt to give axial, shear, and in-plane flexural bonding forces.

For the purpose of this study, only the linear-elastic material response is considered, and the elastic characteristics of the spring-bonds can be described by considering a quarter of element, to which 4 connecting devices are attached, as shown in Fig. 2 where the apex A stands for axial and the apex S stands for shear.

With reference to the regular quarter of element ω^1 shown in grey colour in Fig. 2, the four associated generalized stiffness, or elastic moduli, to obtain the spring stiffness are indicated by k_x^A, k_y^A, k_x^S, k_y^S, and are defined by balancing the elastic energy of 3 basic deformed conditions of the discrete assemblage with the elastic energy of the unit-cell made by a corresponding orthotropic continuum, while for the case of distorted elements these stiffnesses are modified as described in Casolo [28]. This aspect has little relevance when remaining into the linear-elastic field, and in any case the elements of the mesh adopted here are for the most part almost rectangular with the sides aligned with the material reference axes. Moreover, the discretization is at a scale quite coarser than the individual blocks size, and thus the block units are much smaller than the discretized elements, the micro-structure effects tend to become averaged, and the proposed model does not need to apply a specific strategy to account for the flexural in-plane interlocking effects of these elements. The specific values assigned to the axial and shear elastic moduli are explained in Section 4, where it is also reported the mesh of the discretized model (which is plane). The mass of the elements and the stiffness of the connections are assigned taking into consideration the effective thickness of the walls, also considering the contribution of portion of the walls orthogonal to the plane of the analyses, as already done is the case of previous dynamical analyses made on this typology of masonry monuments (Casolo et al. [20]).

The mechanical characteristics of the masonry are defined in the RBSM, as reported in Casolo [28], by considering the following simple equivalence between the elastic moduli of orthotropic Cauchy continuum and the generalized stiffness assigned to the connecting devices: Young's moduli $E_x = k_x^A$, $E_y = k_y^A$ (cfr. Figs. 1 and 2). For the purposes of the study, it seemed acceptable to assume the same Young's modulus in both horizontal and vertical direction: $E_x = E_y$ and hence, $k_x^A = k_y^A$. The link between the shear modulus and the Young's modulus is expressed by Eq. (1):

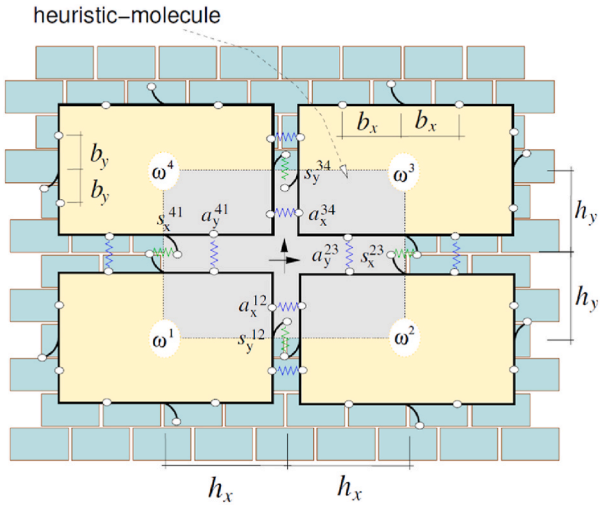

Fig. 1. Schematic representation of a heuristic molecule, RBSM. Differently from the drawing, the mathematics refers to an initial length of the spring that is null.

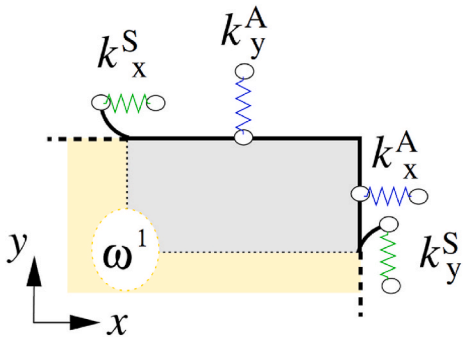

Fig. 2. Schematic representation of a quarter of heuristic molecule, with the quarter of rigid unit (grey) and the corresponding bond-springs.

$$k^S \approx 2G = \frac{E}{n} \tag{1}$$

where the coefficient n is introduced to represent the ratio between the Young's modulus and the double of the shear modulus, which in a homogeneous isotropic elastic material takes the value of $1+\nu$, being ν the Poisson's coefficient.

3.2. Probabilistic characterization

The second step of the process here proposed is the probabilistic characterization of the system. This step becomes crucial when it is necessary to consider different sources of uncertainty, as in the case of historical constructions. In such systems, uncertainties arise both from the prediction model (*i.e.* parameter uncertainty, model inadequacy and code uncertainties and from the measurements (*i.e.* observation error). The objective is to find a vector of the unknown parameters of the numerical model that produces an output consistent with the (experimental) observed data. In this context, the application of the Bayesian approach is spreading in the civil engineering field as a promising solution for increasing the reliability of the computational models (see *e.g.* Beck and Katafygiotis [29], Beck et al. [30], Rocchetta et al. [31], Pepi et al. [32], Murano et al. [33], Ierimonti et al. [34], Monchetti et al. [35]), as well as for overcoming the classical deterministic procedure, which could not ensure the uniqueness and the stability of the solution.

In general terms, the uncertainty quantification problem can be formulated by using the terminology of Kennedy and O'Hagan [36], Arendt et al. [37] and Brynjarsdóttir and O'Hagan [38]. Consider a numerical mechanical model M characterized by the vector of unknowns $\xi = (\varphi_1, \ldots, \varphi_n, \theta_1, \ldots, \theta_m) \in R^{n+m}$ consisting in n latent variables (φ) and m independent unknown parameters (θ). The difference between these two terms is of key importance. The vector θ collects unknown and unobservable quantities whose prior distribution is the object of the inference process. The vector φ collects the latent variables that appear as unknown and unobserved quantities introduced to represent sources of uncertainty that influence the system behaviour. Let assume k observations of the physical system are known, denoted by the vector $d = (d_1, \ldots, d_i, \ldots, d_k)$. These represent observable random variables whose generative process can be reproduced through the numerical model. However, data are always collected with some random measurement errors and no model is perfect. Due to this consideration, the following formulation can be introduced:

$$d = \eta(\xi) + b + \epsilon \tag{2}$$

where d – the observed data – is considered as the result of three terms, the numerical model output $\eta(\xi)$, the model inadequacy b, and the random observation error ϵ. It is worth noticing that Eq. (2) represents the reality through the results of the numerical model and the acquisition of the experimental data. As no model is perfect and no

experimental measurement is flawless, the model inadequacy and the observation error are thus introduced to link the reality to the numerical model result. More in detail, by indicating with D the reality – *i.e.* the real but unknown behaviour of the system –, Eq. (2) become: $d = D + \epsilon = \eta(\xi) + \mathrm{b} + \epsilon$, where $D = \eta(\xi) + \mathrm{b}$.

In this framework, the Bayesian interpretation allows to infer the model parameters on the base on the observed data by including both the degree of belief attributed to a certain quantity and the effect of different sources of uncertainties involved in the process. Indeed, the application of the Bayes' theorem provides the posterior probability distribution of the unknown model parameters ξ, $p(\xi|d, M)$, given the observations (d):

$$p(\xi|d, M) = c_0 \cdot p(d|\xi, M) \cdot p_0(\xi|M) \tag{3}$$

In Eq. (3), $p_0(\xi|M)$ denotes the prior probability density function. $p(d|\xi, M)$ represents the likelihood function. c_0, called the evidence, is a normalizing factor necessary to ensure that the integral of the posterior distribution equals one. Note that, for the sake of simplicity, the conditioning on the model class M is dropped hereafter (Box and Tiao [39]).

The prior distribution represents the current information about unknowns before the data d are available. The initial knowledge of the true values of the ξ-parameters is thus quantified in terms of their prior distribution and then updated on the basis of the new available observations. The likelihood function expresses the probability of obtaining the model output corresponding to the experimental data d given certain values of ξ. This term can be interpreted as a measure of the effectiveness of the numerical model in reproducing the observations. It contains, on the one hand, the function through which the current data modifies prior knowledge and, on the other hand, the information about the unknown parameters coming from the observations. From Eq. (2), d is a random vector whose randomness is caused by the randomness of the observation error and the model inadequacy. The probability density function of this random vector, $p(d|\xi)$, can be achieved as the convolution of two probability distributions following the total probability theorem:

$$p(d|\xi) = \int p(d|D, \xi) p(D|\xi) dD = \int p(d|D) p(D|\xi) dD \tag{4}$$

The likelihood function is thus obtained as the result of the integral of Eq. (4) which is solved through the convolution of the observation and modelling errors distributions. When the number of parameters to be inferred is low, the continuum joint-space of the ξ-parameters can be discretized and only the parameter values leading to a pseudo-dataset congruent to the observed data can be considered, according to the selected observation error. In doing so, the updating framework is conducted through a direct integration of the likelihood function by rounding a continuous problem to a discrete problem. The integrals representing the likelihood function and the normalizing factor are thus solved via numerical solution and the large number of required simulations can be reduced by using the Latin Hypercube sampling technique (see *e.g.* Monchetti et al. [10]). It is worth noticing that this procedure represents a simplification of the problem, also because, in some applications, the number of parameters to be inferred may be higher. In the following, the probabilistic characterization of the prior observation error, the parameter uncertainty, and the model inadequacy are introduced as possible choices for the terms involved in the Bayesian Uncertainty Quantification (Cheung and Beck [40], Goller and Schuëller [41], Rocchetta et al. [31]).

Observation error. Observations are collected to investigate the actual system response but, as previously mentioned, this operation includes some uncertainties, for instance, those related to instrument error. In the context of the present research, observations are referred to the evaluation of the natural frequencies of the structure. As a first assumption, all the different causes which could lead to an incorrect evaluation of the modal characteristics, are assumed as equally relevant and substantially non-dependent from the values of the frequency itself. The observation errors ϵ_i are hence defined as *i.i.d.* $N(\mu, \sigma^2)$ with zero mean.

$$p(d|D, \xi) \propto exp\left[\frac{-1}{2}\frac{(D-d)^2}{\sigma^2}\right] \tag{5}$$

This PDF is used as the first term of the likelihood function in Eq. (4).

Parameter uncertainty. The parameter uncertainty is related to all the uncertainties entering as inputs in the numerical model. This contribution reflects the initial knowledge about the model parameters, and in Eq. (3), it is recognized through the prior distribution. At the present stage of the research, one updating parameter is proposed: the coefficient n. This parameter, introduced in Eq. (1), represents the ratio between the Young's modulus and the double of the shear modulus. Note that the value of the Young's modulus has been considered as latent variable. For the purpose of the present research, to represent the variability range of these mechanical characteristics of masonry, lognormal PDFs can be selected as suggested in CNR [42], Bosiljkov et al. [15] and, Tomaževič [4]. These properties, as a first instance, are considered homogeneous along the structure.

Model inadequacy. For the purpose of defining this contribution, it is significant to underline that despite the true values of the input model parameters being known, a discrepancy between the model output and its actual value should be taken into account (Kennedy and O'Hagan [36]). This source of uncertainty can be considered as a probability distribution of the model output $\eta(x_i, \boldsymbol{\xi})$, given a set of input parameters $\boldsymbol{\xi}$. In this paper, the RBSM is selected to represent the dynamic features of the system and a nuisance parameter, which affects the model output, is introduced to reflect the potential dispersion of the calculated natural frequencies. Starting from the definition of a PDF for the nuisance parameter, the variability of the model output is evaluated as a PDF too, in terms of frequencies. It is worth noting that this term represents the second contribution of the likelihood function presented in Eq. (4) and its crucial role was underlined in Brynjarsdóttir and O'Hagan [38] by demonstrating that an analysis that does not account for model discrepancy may lead to biased and over-confident parameter estimates and predictions.

4. Selected masonry tower

Three existing masonry towers are here comparatively analysed: (a) the *Giotto*'s bell tower (Florence, Italy), (b) the *Matildea* tower (Bondeno, Italy) and (c) the *Rotella* tower (Ascoli Piceno, Italy). Defining the slenderness as the ratio of the tower height (H) to its lateral dimension (L), i.e., the cross-sectional dimension, the three selected towers exhibit different slenderness values, equal to 6, 4, and 3, respectively (Fig. 3).

The geometry of the towers is obtained from existing available documentation including cross-sections, front and planar views. These data as well as the results of the experimental campaign are reported in: Lacanna et al. [23] and Spinelli et al. [43] for the tower (a), Standoli et al. [24] for the tower (b), Ferrante et al. [26] for the tower (c).

The choice of masonry towers, among all the typologies of heritage structures, is closely related to their structural simplicity, which allows for the successful employment of a plane RBSM. Nevertheless, as the proposed methodology aims at analysing the influence of shear deformability, the field of application should be limited to "squat" towers, characterized by a slenderness less than or equal to 5. It is for such cases that the shear modulus of the masonry affects the natural frequencies and mode shapes, making this parameter effective the model updating. The *Matildea* tower (b) and the *Rotella* tower (c) embody two emblematic case studies which are investigated in depth as representative applications throughout this paper, drawing out the potential of the proposed procedure to update the value of the ratio between Young's modulus and shear modulus. On the contrary, the discussion of *Giotto's* bell tower, characterized by a slenderness ratio greater than 5, will show that when the method is applied to particularly slender structures, it does not allow the identification of the effects associated with the shear modulus.

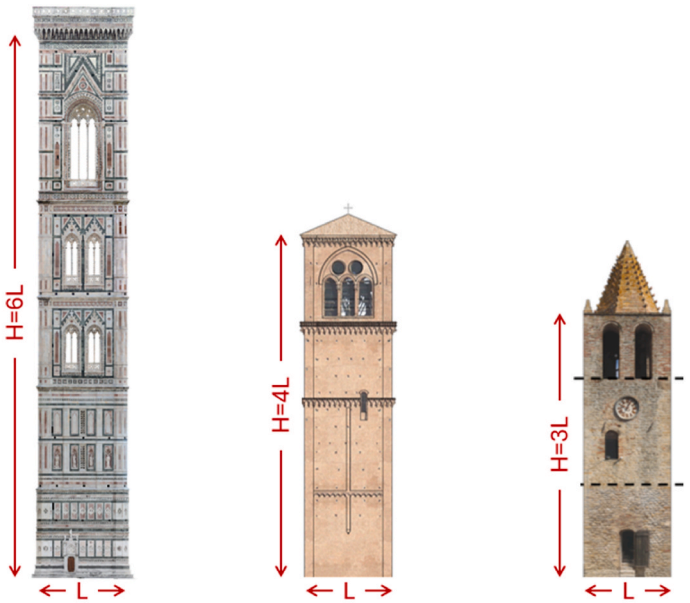

tower	(a)	(b)	(c)
L [m]	13.00	7.20	4.60
λ [−]	6	4	3

Fig. 3. Main characteristics of the three towers: (a) Giotto's bell tower, (b) Matildea tower, and (c) Rotella tower.

4.1. Geometric data

The relevant geometrical features of the three considered towers are schematically compared in Fig. 3. A concise description of each structure is reported in what follows.

(a) The *Giotto*'s bell tower is a masterpiece of the Italian Gothic. It was completed in 1359. It has a square base of about 13 m on each side (without considering the angular spurs) and a total wall thickness of about 3.30 m (including the marble covering). The total height is 84.7 m above ground. The exterior is entirely clad in white, red and green marble, the inner face of the supporting walls is built with a well-dressed stone with regular and squared blocks, and the mortar joints are thin.

(b) The construction of the *Matildea* tower started around the XII century and continued until XV century. Its height, at the beginning 12 m, raised up until 30 m with the construction of the bell cell. The structure, which at the base unveils the typical medieval layout, shows the late Gothic style in the bell cell. The tower has a square cross-section with sides of 7.2 m long which remain constant until the top of the tower. The walls of the tower, made of solid bricks, have a double case structure that hosts the stairs in the zone between the two wall layers. The external wall thickness is around 1.05 m up to 14.8 m elevation, before decreasing to 0.9 m until the top of the tower. The inner wall layer has a constant thickness equal to 0.45 m. As far as the restraint conditions provided by the adjacent Maria Vergine church (Standoli et al. [24]) underlines that the *Matildea* tower may be considered as an isolated construction due to the weak connection between these two constructions.

(c) The *Rotella* tower goes back to the XI century; recently, it suffered significant damage after the Central Italy seismic sequence of 2016. The structure of the tower is composed of a rectangular cross section with dimensions equal to 4.60 m × 4.65 m. The multi-leaf masonry walls are characterized by a thickness equal to 1 m. The total height of the tower is about 17.60 m, and along its vertical development does not present any relevant variation of their geometry. The tower has multi-leaf masonry walls characterised by bricks and stones of different sizes, which are irregularly arranged in the panels.

The experimental results in terms of main natural frequencies were obtained through Operational Modal Analysis (OMA) and are reported in Lacanna et al. [23], Standoli et al. [24] and Ferrante et al. [26]. For the sake of clarity, they are herein summarized in Table 1, where the first and the fourth bending frequency (the second along the considered direction) are considered.

From now on, focusing the interest on the first two bending frequencies in a direction, the first frequency reported in Table 1 will be denoted as f_1^{exp}, while the fourth frequency (that is the second bending frequency along the direction of interest) will be denoted as f_2^{exp}.

4.2. Computational model

The RBSM is employed to perform eigenvalue analyses of the three analysed towers. This is a simplified 2D discretization of the towers, see Fig. 4. This discretization is obtained by means of quadrilateral rigid elements, with the mass concentrated in the centroid, interconnected by non-linear shear and axial springs. The geometry of the RBSM is described by considering a global Cartesian coordinate system oriented with the *x*-axis parallel to the bed-joints. This geometrical domain is divided into quadrilateral elements so that no vertex of a generic quadrilateral lies on the edge of another quadrilateral. The dimension of the quadrilateral rigid element is about 0.6-0.8 m, but some smaller elements were necessary to accurately reproduce the peculiar geometry of the towers. The computational models of the three towers considered differ from numbers of nodes and elements; in particular: the bell tower

Table 1
Experimental frequencies.

Mode # i	*Giotto*'s tower f_i [Hz]	*Matildea* tower f_i [Hz]	*Rotella* tower f_i [Hz]	Mode type
1- f_1^{exp}	0.65	1.48	2.68	Bending
4- f_2^{exp}	3.16	4.99	9.38	Bending

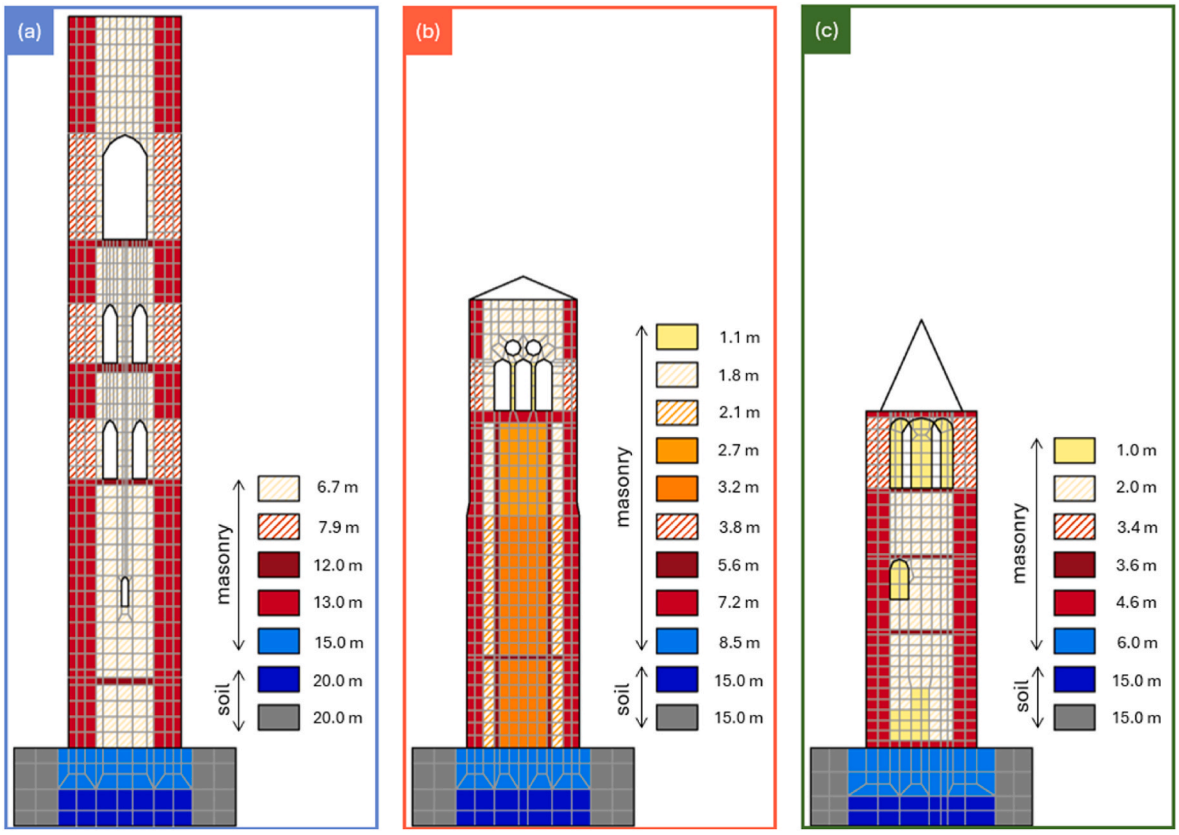

Fig. 4. RBSM model (left) and thickness (right): (a) Giotto's bell tower, (b) Matildea tower, and (c) Rotella tower.

of *Giotto* is discretized into 1060 nodes and 923 quadrilateral rigid elements; the *Matildea* tower into 634 nodes and 554 quadrilateral rigid elements, and the *Rotella* tower into 509 elements and 838 quadrilateral rigid elements. Different thicknesses are assumed for the elements to reproduce – even with a 2D representation – the three-dimensional geometrical configuration of the towers. They are indicated in Fig. 4 by different colours. The direction chosen for the analyses corresponds to the main façade of the towers. For a comprehensive description of the role of wall thickness within the RBSM approach, the interested reader is referred to Casolo [44].

With the aim to investigate the convenience to infer the shear modulus of the masonry by using the experimental observations of the natural frequencies of the towers, sensitivity analyses are performed. Different values of Young's modulus (ranging from 1000 to 5000 MPa) and coefficient n (ranging from 1 to 5) are considered. The results, in terms of natural frequencies, are shown in Fig. 5 (for the first bending frequency) and Fig. 6 (for the second bending frequency).

The results show that the Young's modulus has a strong influence on the natural frequencies (as clearly expected); however, the coefficient n also appears to play a role, particularly for the second bending frequency and with decreasing tower slenderness. This aspect encourages the effort to examine in depth the Bayesian Uncertainty Quantification to infer the shear modulus of the masonry in the RBSM field by using dynamical observations because it deals with the combination of two challenging aspects. On the one hand, the evaluation of the shear modulus through non-invasive observations, and on the other hand, the handling of the uncertainties in the definition of this mechanical parameter.

5. Bayesian shear modulus quantification

In this section, all the terms involved in the Bayesian UQ are reported, and the results for the three tower case studies are discussed. As mentioned in Section 3, only one updating parameter is selected: the coefficient n. The first and second natural bending frequencies are used to reference and reported in Table 1.

Set $d = \{f_1^{exp}, f_4^{exp}\}$ as observations vector, the posterior marginal

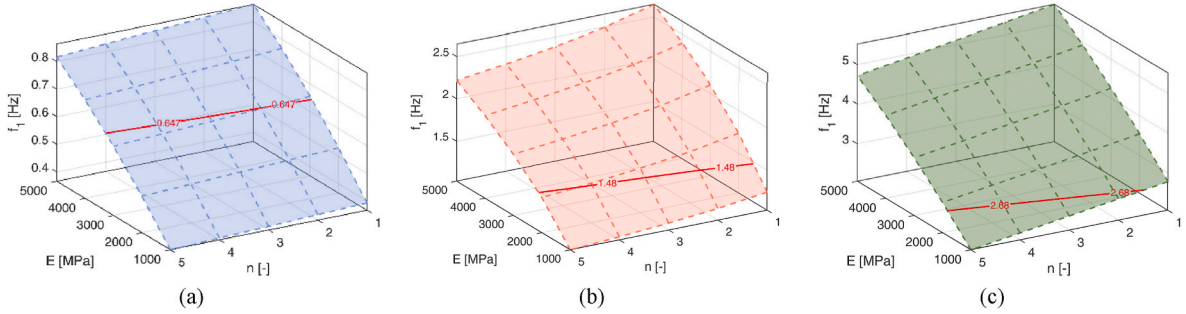

Fig. 5. First bending frequency as function of the Young's modulus and coefficient n in the case of (a) *Giotto*'s bell tower, (b) *Matildea* tower, and (c) *Rotella* tower. The contour line represents the experimental data f_1^{exp}.

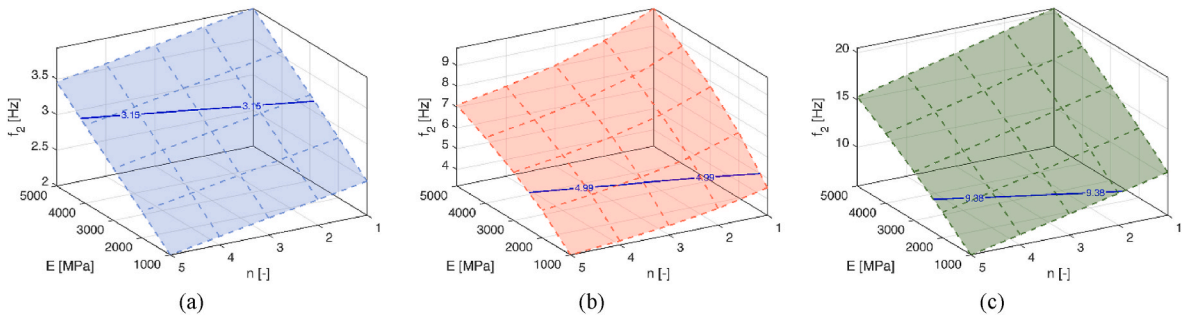

Fig. 6. Second bending frequency as function of the Young's modulus and coefficient n in the case of (a) *Giotto*'s bell tower, (b) *Matildea* tower, and (c) *Rotella* tower. The contour line represents the experimental data f_2^{exp}.

PDF of the coefficient n can be evaluated with. Eqs. (3) and (4). More in detail, the observation errors are computed through *i.i.d.* $N(f_i^{exp}, 0.02^2)$, Eq. (5), whereas the modelling errors are included in the process by taking into account a nuisance parameter which affects the model output. It is worth noticing that this assumption on the observation errors represents a simplification of the problem. Even though, it is conventionally used in literature (Simoen et al. [45], Yuen [46], Behmanesh et al. [47]), the error uncertainties are usually unknown, and a better quantification of these functions might lead to a more reliable estimation of the posterior distribution.

It is worth noting that in the current formulation of the problem the variance was selected as a fixed value, consistent with previous Bayesian OMA applications and with the typical scatter observed in experimental modal frequencies based on the authors' experience. However, OMA-based modal identification procedures, at least in general terms, yield mode-dependent uncertainties, which are often larger for higher modes. Consequently, future developments of this approach, supported by a larger dataset in terms of masonry tower geometric characteristics and experimental results, may consider jointly inferring the error variance together with the model parameters and exploiting identification-based confidence bounds.

In this application, the Young's modulus is considered as the latent variable by taking into account a lognormal distribution with a mean equal to 1800 MPa and a standard deviation of logarithmic values equal to 0.06. The modelling errors are thus originated through the uncertainties related to the level of knowledge on the Young's modulus and computed based on the model output dispersion, in terms of natural frequencies. The likelihood function so defined, represents therefore the goodness of fit of the computational model to the observation data by including the information on the uncertain parameters. Note that the definition of the likelihood function would be demanding because requires numerical approximation of the integral of Eq. (4), based on multiple runs of computational model. A Latin Hypercube Sampling technique was employed, thus reducing to about 200 the number to simulations needed to reproduce the continuum joint-space. This sampling technique represents a simplification of the problem which is frequently applied when the dimension of the vector of unknowns is limited. The prior distribution of the coefficient n is here selected through the lognormal PDF shown in Fig. 7 to represent a subjective choice of the random variable, on the basis of the authors' judgment. This distribution, with a mean equal to 2.2 and a standard deviation of logarithmic values equal to 0.2, seeks to reproduce the extremely scattered value of the ratio between shear modulus and Young's modulus reported in the scientific literature (Tomaževič et al. [48], Tomaževič [4], Croce et al. [17]).

In Fig. 7, in addition to the graphical representation of the prior distribution of the coefficient n, two dotted lines are reported to highlight two reference values of the ratio between shear modulus and Young's modulus. The first corresponds to the recommendation in Eurocode 6 (CEN [16]), which indicates to evaluate the shear modulus

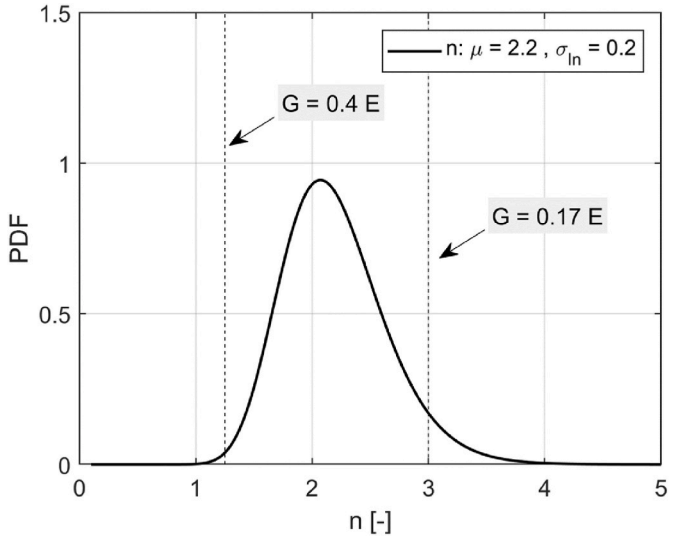

Fig. 7. Prior lognormal distribution of the coefficient n.

based on the Young's modulus as $G = 0.4E$. This relation is obtained by setting the Poisson's coefficient of the masonry, ν, to 0.25 in the formula linking the elastic constants in isotropic materials, $G = E/[2(1+\nu)]$. The second reference value, $G = 0.17E$ instead, is a common assumption in the seismic assessment of masonry buildings field (Croce et al. [17]). This latter relation gathered from experimental value of the ratio between shear modulus and Young's modulus which can vary, as reported in Tomaževič et al. [48] and Tomaževič [4], between 0.06 and 0.25. The results of the proposed Bayesian updating are summarized in Figs. 8 and 9, and Table 2. In particular: Fig. 8(a)–(c) and (e) shows the results of the Bayesian updating by using the prior PDF reported in Fig. 7 and the experimental observation of the first bending frequency of *Giotto*'s tower, *Matildea* tower and *Rotella* tower, respectively. Fig. 8(b)–(d) and (f) shows the results obtained by using the same prior PDFs but the experimental observation of the second bending frequency of *Giotto*'s tower, *Matildea* tower and *Rotella* tower, respectively. Fig. 9(a) and (b) and (c) shows, on the other hand, the second step of the Bayesian updating by using as prior PDF the posterior PDF reported in the first column of Fig. 8 and the experimental observation of the fourth frequency (the second in the façade direction) of *Giotto*'s tower, *Matildea* tower and *Rotella* tower, respectively. The coefficient n posterior PDF of the first updating step is quite similar to the prior PDF, by indicating that the first natural frequency is non informative with respect to this parameter. This aspect confirms the outcomes achieved from the sensitivity analyses (see Fig. 5). The more compelling results, instead, are related to the second updating step for the squat towers (*i.e.* the *Matildea* tower and the *Rotella* tower). In these cases, as we can see in Fig. 9(b) and (c), the observation of the second bending frequency

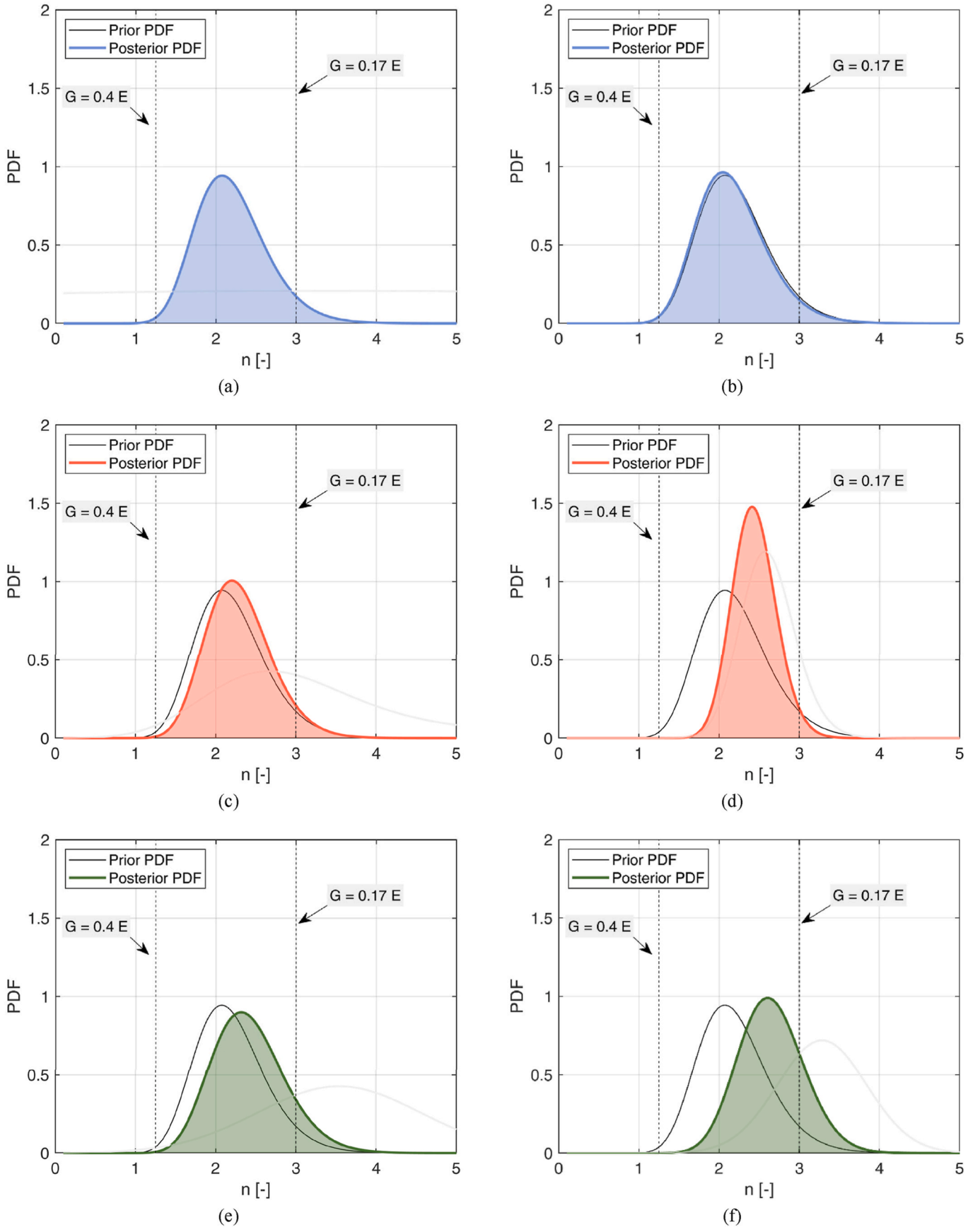

Fig. 8. Posterior distributions of the coefficient *n*. On the left, updating with the first bending frequency of (a) *Giotto*'s tower, (c) *Matildea* tower and (e) *Rotella* tower. On the right, updating with the second bending frequency of (b) *Giotto*'s tower, (d) *Matildea* tower and (f) *Rotella* tower. The light grey curves represent the likelihood functions.

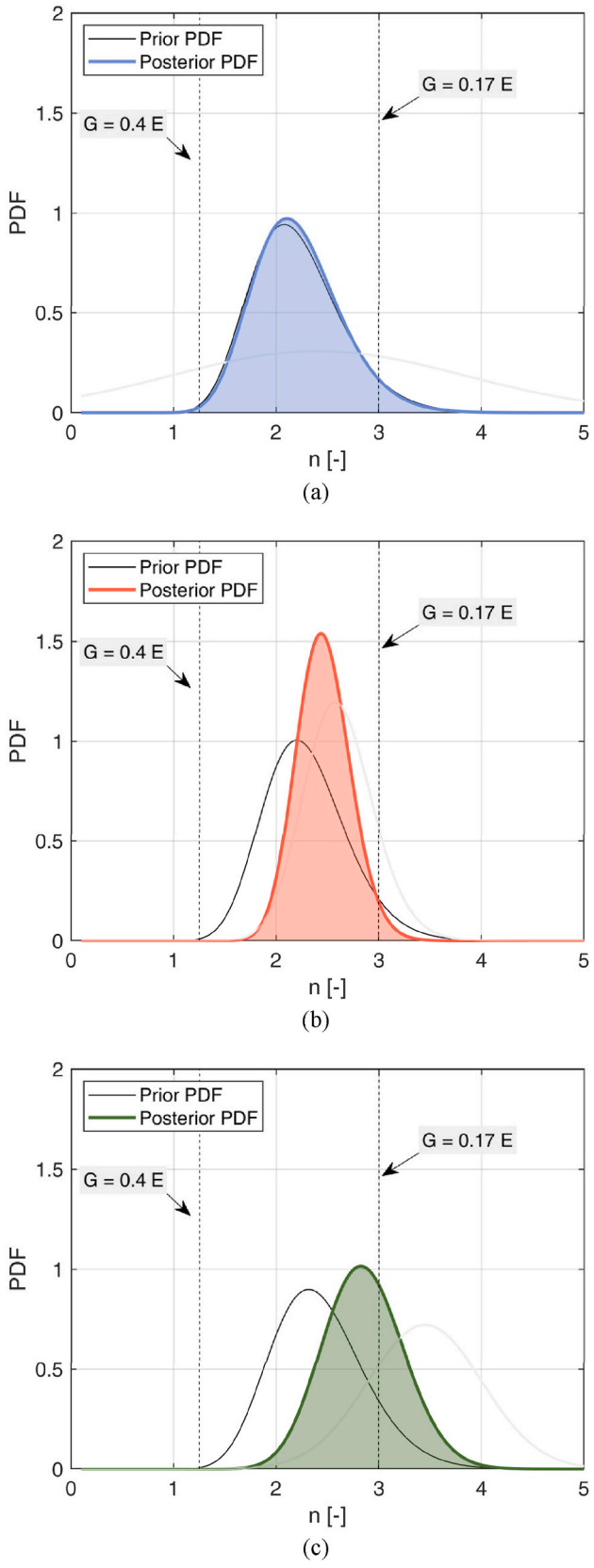

Fig. 9. Posterior distributions of the coefficient *n*. Updating with the first two bending frequencies of (a) *Giotto*'s tower, (b) *Matildea* tower and (c) *Rotella* tower. The light grey curves represent the likelihood functions.

Table 2
Mean value and standard deviation of logarithmic value of prior and posterior distributions of coefficient *n*. Note that, "step 1 (f_1^{exp})" is related to the updating performed with the first bending frequency, "step 1 (f_2^{exp})" is related to the updating with the second bending frequency and "step 2" includes the updating with the first and the second bending frequency.

tower	PDF parameters	Prior PDF	Posterior PDF step 1 (f_1^{exp})	Posterior PDF step 1 (f_2^{exp})	Posterior PDF step 2
(a)	μ	2.20	2.20	2.20	2.20
	σ_{ln}	0.20	0.20	0.20	0.20
(b)	μ	2.20	2.30	2.70	2.75
	σ_{ln}	0.20	0.18	0.13	0.11
(c)	μ	2.20	2.50	2.82	2.95
	σ_{ln}	0.20	0.21	0.17	0.15

significantly change the posterior PDF compared to the prior PDF, both in terms of mean and standard deviation (Table 2). The same trend can be observed in Fig. 8 (d) and (f) where only the second experimental frequency is used as data set in the updating procedure. This is not unexpected, as Figs. 5 and 6 already showed that the coefficient *n* plays an increasing role in the second bending mode, which becomes more evident as tower slenderness decreases. The achievements gain with the Bayesian inference herein proposed, move in the direction also suggested by Tomaževič et al. [48], Tomaževič [4] and Croce et al. [17] and here obtained through the Bayesian UQ by using the observation of natural frequencies of squat masonry towers by employing RBSM.

5.1. Discussion of the results

In order to point out the outcomes of the proposed approach, a comparison between the Finite Element (FE) model and the RBSM is reported. The geometrical configuration of the three towers, represented in Fig. 4, is used to define a two-dimensional FE model by using the commercial code SAP2000. For the Young's modulus of the masonry, a range of values varying from 500 MPa to 4000 MPa, is considered. Since a linear elastic isotropic material model is adopted, the ratio between the shear modulus and the Young's modulus remains constant, as it is defined by fixing the Poisson's ratio to 0.25 through the constitutive relationships of isotropic materials.

The results of the modal analyses, in terms of natural frequencies, obtained from the FE model are reported on the left-hand side of Fig. 10 for each of the considered towers. It is noteworthy that none of the assumed Young's modulus values is able to simultaneously reproduce both the first and second frequencies, except in the case of *Giotto's* tower, for which the difference between the two corresponding values is around 150 MPa. For the *Matildea* tower and the *Rotella* tower, this difference is more pronounced. In the case of the *Matildea* tower, the first natural frequency is matched with a value of the Young's modulus equal to 1590 MPa, whereas the second natural frequency is matched by a Young's modulus of 1270 MPa. For the *Rotella* tower, these two values are equal to 980 MPa and 735 MPa, respectively, for the first and the second natural frequency. Let us assume a lognormal distribution for the Young's modulus, with a mean equal to the value matching the first natural frequency of each tower in the FE model and a standard deviation equal to the target value suggested by CNR-DT 212/2013 (CNR [42]). Under this assumption, the Young's modulus value matching the second natural frequency in the analysed direction corresponds to the 55th, 20th and 18th percentiles of the distribution for the *Giotto*'s tower, *Matildea* tower and *Rotella* tower, respectively.

On the right-hand side of Fig. 10, the scatter between the Young's moduli matching the two natural frequencies for the three towers is shown by red and blue dots on the lognormal distribution and can be interpreted as a measure of the FE modelling error.

A relevant aspect emerges when these results are compared with the outputs of the RBSM; Fig. 11 reports the comparison between the outputs of the FE model (dotted black lines) and RBSM (continuous line) in

terms of the first (light blue lines) and second frequency (orange lines) of the three towers. The results of the RBSM are represented for different values of the Young's modulus, ranging from 500 MPa to 4000 MPa, and for different values of the coefficient n, ranging from 1 to 4. What emerges clearly is that the RBSM can reproduce simultaneously both the first and the second frequency for the two considered squat towers; in

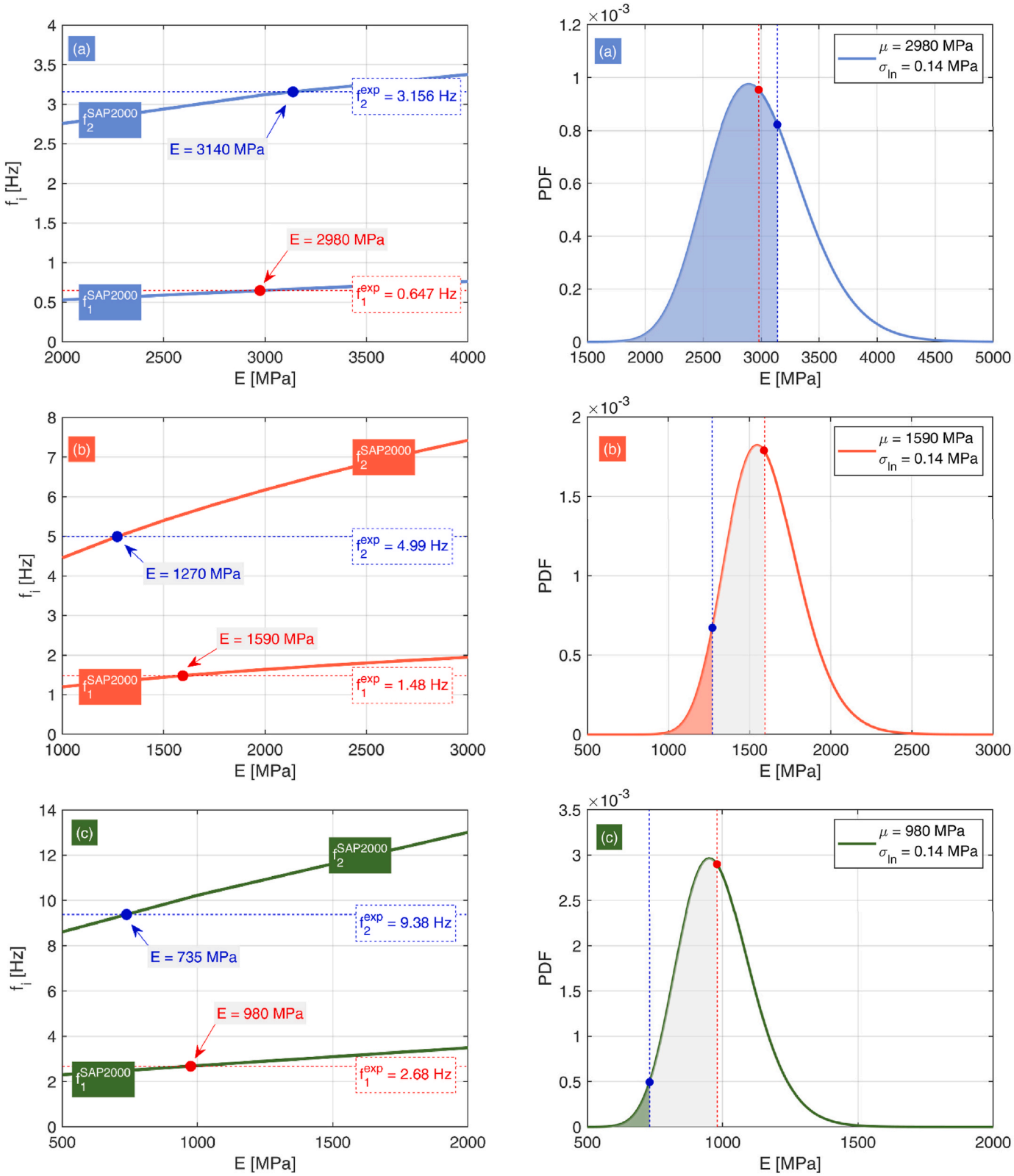

Fig. 10. On the left, the results in terms of frequencies of the FE model of the *Giotto*'s tower (a), *Matildea* tower (b) and *Rotella* tower (c). On the right, lognormal distribution with mean equal to the value that matches the first natural frequency of the towers with FE model, and the standard deviation value equal to one suggested in CNR-DT 212/2013 (CNR [42]).

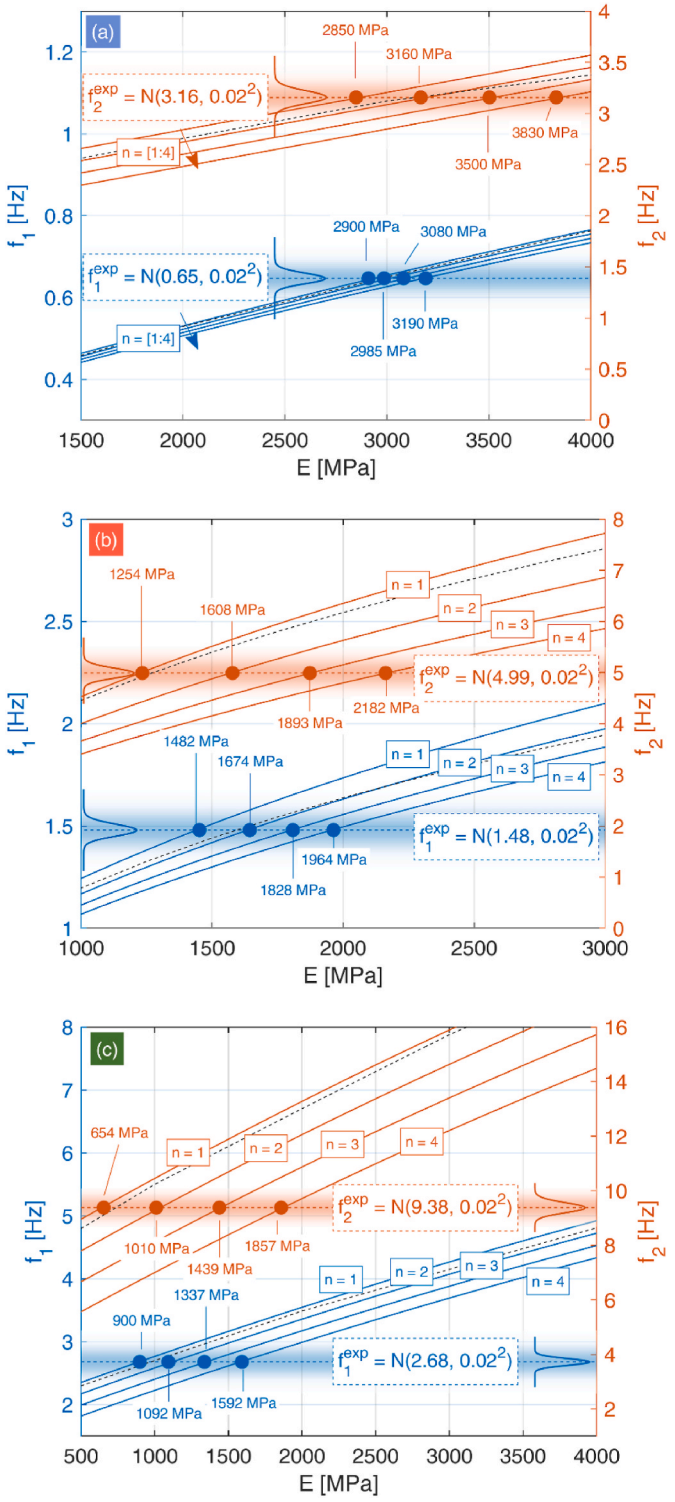

Fig. 11. Comparison between FE model (represented by the dotted black line) and RBSM (represented by the blue and orange continuous lines) results in terms of natural frequencies for the *Giotto*'s tower (a), *Matildea* tower (b) and *Rotella* tower (c). The figures show two y-axes: on the right in blue the first frequency, and on the left in orange the second frequency. Note that, with continuous blue and orange curves are represented the measurement uncertainty PDF of f_1^{exp} and f_2^{exp}. (For interpretation of the references to colour in this figure legend, the reader is referred to the Web version of this article.)

other words, it is possible to define a pair of values (Young's modulus and coefficient n) that satisfies the experimental observations.

However, as discussed throughout the paper, no experimental data are free from uncertainties and no model is perfect. To clarify this aspect, uncertainty bands and the corresponding probability distributions have been included in the figure for each experimental data. These uncertainty bands, if analysed with the variability of the elastic modulus (represented on the x-axes of Fig. 11), allow to critically evaluate the effect of modelling and measurement uncertainty that are included in the likelihood function. On the one hand, the variability of the measurement error can be observed with the blue and orange uncertainty bands for the first (f_1^{exp}) and second (f_2^{exp}) bending frequency, respectively. On the other hand, the modelling error has been included as latent variable of the elastic modulus of the masonry; and its effect can be observed on the x-axes of Fig. 11 for both the computational model considered.

By comparing Fig. 11 with the results of the Bayesian UQ, reported in Fig. 8 and Tables 2 and it emerge that the target values of the coefficient n converge to approximately 1.25 for the *Giotto*'s tower and to about 2.75 for the two squat towers considered: the *Maltildea* and *Rotella* towers. This implies that, for squat masonry towers, simultaneously satisfying both observations requires a value of the coefficient n that violates the assumption of isotropic masonry behaviour. This latter result sets the ratio between the shear modulus (G) and the Young's modulus (E) equal to 0.18. In doing so, it approaches the values proposed in literature by Tomaževič et al. [48], Tomaževič [4] and – more recently – Croce et al. [17], while deviating from the value currently reported in Eurocode 6 (CEN [16]), which is based on representing masonry as an isotropic material. It is worth noting that this result was obtained, on the one hand, by overcoming the standard isotropic approach based on the Cauchy solid continuum through the adoption of a fully discrete modelling strategy (the RBSM) and, on the other hand, by developing a Bayesian UQ procedure based on experimental frequency data.

With respect to the RBSM computation approach, it has to be reported that the adoption of a two-dimensional modeling framework inevitably entails limitations in the representation of the full dynamic behavior of masonry towers. In particular, torsional modes cannot be reproduced within a 2D formulation and are therefore excluded from the present analysis and from the associated Bayesian inference procedure. This limitation is here explicitly acknowledged and specifies the scope of this present work. Within the two-dimensional framework, only the first two bending modes were considered. This choice was motivated by both practical and experimental considerations. From an experimental standpoint, these modes are typically the easiest to be identified, especially in long-term monitoring, as they are most readily activated by ambient excitations. In addition, higher-order bending (or torsional) modes were not observed, or were not available, in the experimental dataset employed for this study. Despite these modeling simplifications, the results highlight a relevant physical aspect with direct implications also for engineering practice, namely the potential inadequacy of assuming an isotropic masonry behavior with code-prescribed values of the G/E ratio. The findings indicate that, particularly for squat masonry towers, the shear response may significantly influence the dynamic behavior, leading to values of the coefficient n that deviate from those commonly adopted in design practice. This potentially affects both the modal updating procedure and the results of time-history analyses. Thus, while the present study does not aim to provide prescriptive design recommendations, it suggests that neglecting non-isotropic effects may result in an incomplete characterization of the structural response especially in case of squat masonry towers. This observation motivates further research on the role of shear stiffness in masonry towers and its implications for the modelling assumptions adopted in practical design.

The findings of this paper, by the way, considering the invasive nature of the experimental tests required for the direct evaluation of the masonry shear modulus, show that, in the case of squat masonry towers,

Bayesian inference based on experimental frequency data allows for a reliable estimation of the shear modulus.

6. Concluding remarks

To update the shear parameter of masonry towers, this paper combines the anisotropic modelling capability of the RBSM with Bayesian inference based on dynamic experimental data. After setting up the methodology (both material and methods), the approach is applied to a representative set of case studies comprising both slender and squat masonry towers, highlighting the main advantages of the proposed framework as well as its limitations. To address Bayesian inference, as updating parameter was selected the ratio between the Young's modulus and twice the masonry shear modulus (denoted here as the coefficient n). This parameter was updated using experimental observations of two bending frequencies. The results obtained using the RBSM approach were compared with those obtained using a conventional FE modelling technique based on the assumption of isotropic masonry behaviour. The adopted Bayesian model updating procedure allows for the estimation of the masonry shear modulus while accounting for uncertainties, and the comparison shows that, for squat masonry towers, satisfying both observations simultaneously requires a combination of Young's modulus and coefficient n that violates the assumption of isotropic masonry behaviour. This finding, which is consistent with the well-known anisotropic behaviour of masonry extensively investigated in the scientific literature, has the merit of rigorously specifying the key role of the masonry shear modulus in model identification and, consequently, in the reliability of computational models. Finally, it is worth noting that, since this behaviour has been observed for squat masonry towers, Bayesian inference based on frequency data can be considered a reliable method for estimating the shear modulus in such structures, as an alternative to traditional and invasive experimental methods.

CRediT authorship contribution statement

Silvia Monchetti: Writing – review & editing, Writing – original draft, Methodology, Formal analysis, Data curation, Conceptualization. **Gianni Bartoli:** Writing – review & editing, Writing – original draft, Conceptualization. **Michele Betti:** Writing – review & editing, Writing – original draft, Conceptualization. **Siro Casolo:** Writing – review & editing, Writing – original draft, Software, Methodology, Conceptualization. **Francesco Clementi:** Writing – review & editing, Writing – original draft, Resources.

Declaration of competing interest

The authors declare that they have no known competing financial interests or personal relationships that could have appeared to influence the work reported in this paper.

Acknowledgements

This project is supported by Spoke 7 (Protection and Conservation of Cultural Heritage Against Climate Changes, Natural and Anthropic Risks) Project PE 0000020 CHANGES (Cultural Heritage Active Innovation for Sustainable Society) - CUPB53C22004010006, NRP Mission 4 Component 2 Investment 1.3, funded by the European Union – Next Generation EU.

Data availability

Data will be made available on request.

References

[1] S. Cattari, B. Calderoni, I. Caliò, G. Camata, S. de Miranda, G. Magenes, G. Milani, A. Saetta, Nonlinear modeling of the seismic response of masonry structures: critical review and open issues towards engineering practice, Bull. Earthq. Eng. 20 (2022) 1939–1997, https://doi.org/10.1007/s10518-021-01263-1.
[2] NTC 2018, D.M. Del Ministero delle Infrastrutture e dei Trasporti del 17/01/2018. Aggiornamento Delle "Norme Tecniche per le Costruzioni". G.U. n. 42 del 20 febbraio 2018, 2018 (in Italian).
[3] S. Cattari, G. Magenes, Benchmarking the software packages to model and assess the seismic response of unreinforced masonry existing buildings through nonlinear static analyses, Bull. Earthq. Eng. 20 (2022) 1901–1936, https://doi.org/10.1007/s10518-021-01078-0.
[4] M. Tomaževič, Shear resistance of masonry walls and eurocode 6: shear versus tensile strength of masonry, Mater. Struct. 42 (2009) 889–907, https://doi.org/10.1617/s11527-008-9430-6.
[5] S. Boschi, L. Galano, A. Vignoli, Mechanical characterisation of Tuscany masonry typologies by in situ tests, Bull. Earthq. Eng. 17 (2019) 413–438, https://doi.org/10.1007/s10518-018-0451-4.
[6] S. Casolo, L. Biolzi, V. Carvelli, G. Barbieri, Testing masonry blockwork panels for orthotropic shear strength, Constr. Build. Mater. 214 (2019) 74–92, https://doi.org/10.1016/j.conbuildmat.2019.04.116.
[7] M. Betti, L. Galano, Shear strength of rubble stone-and-brick masonry panels. A new proposal for the interpretation of sheppard test results, Constr. Build. Mater. 279 (2021) 121925, https://doi.org/10.1016/j.conbuildmat.2020.121925.
[8] A.M. D'Altri, V. Sarhosis, G. Milani, J. Rots, S. Cattari, S. Lagomarsino, E. Sacco, A. Tralli, G. Castellazzi, S. de Miranda, Modeling strategies for the computational analysis of unreinforced masonry structures: review and classification, Arch. Comput. Methods Eng. 27 (2020) 1153–1185, https://doi.org/10.1007/s11831-019-09351-x.
[9] M. Schiavoni, E. Giordano, F. Roscini, F. Clementi, Numerical modeling of a majestic masonry structure: a comparison of advanced techniques, Eng. Fail. Anal. 149 (2023) 107293, https://doi.org/10.1016/j.engfailanal.2023.107293.
[10] S. Monchetti, C. Viscardi, M. Betti, G. Bartoli, Bayesian-based model updating using natural frequency data for historic masonry towers, Probab. Eng. Mech. 70 (2022) 103337, https://doi.org/10.1016/j.probengmech.2022.103337.
[11] M. Corradi, A. Borri, A. Vignoli, Experimental study on the determination of strength of masonry walls, Constr. Build. Mater. 17 (5) (2003) 325–337, https://doi.org/10.1016/S0950-0618(03)00007-2.
[12] A. Brignola, S. Frumento, S. Lagomarsino, S. Podestà, Identification of shear parameters of masonry panels through the In-Situ diagonal compression test, Int. J. Architect. Herit. 3 (1) (2008) 52–73, https://doi.org/10.1080/15583050802138634.
[13] M. Andreini, A. De Falco, L. Giresini, M. Sassu, Mechanical characterization of masonry walls with chaotic texture: procedures and results of In-Situ tests, Int. J. Architect. Herit. 8 (3) (2014) 376–407, https://doi.org/10.1080/15583058.2013.826302.
[14] A. Borri, G. Castori, M. Corradi, Determination of shear strength of masonry panels through different tests, Int. J. Architect. Herit. 9 (8) (2015) 913–927, https://doi.org/10.1080/15583058.2013.804607.
[15] V.K. Bosiljkov, Y.Z. Totoev, J.M. Nichols, Shear modulus and stiffness of brickwork masonry: an experimental perspective, Struct. Eng. Mech. 20 (1) (2005) 21–43, https://doi.org/10.12989/sem.2005.20.1.021.
[16] CEN, Eurocode 6: Design of Masonry structures—part 1-1: Common Rules for Reinforced and Unreinforced Masonry Structures, 2005. EN 1996-1-1:2005. Brussels.
[17] P. Croce, M.L. Beconcini, P. Formichi, P. Cioni, F. Landi, C. Mochi, F. De Lellis, E. Mariotti, I. Serra, Shear modulus of masonry walls: a critical review, Procedia Struct. Integr. 11 (2018) 339–346, https://doi.org/10.1016/j.prostr.2018.11.044.
[18] S. Casolo, Macroscale modelling of the micro-structure damage evolution by a rigid body and spring model, J. Mech. Mater. Struct. 4 (3) (2009) 551–570, https://doi.org/10.2140/jomms.2009.4.551.
[19] T. Kawai, New discrete models and their application to seismic response analysis of structures, Nucl. Eng. Des. 48 (1) (1978) 207–229, https://doi.org/10.1016/0029-5493(78)90217-0.
[20] S. Casolo, G. Milani, G. Uva, C. Alessandri, Comparative seismic vulnerability analysis on ten masonry towers in the coastal Po valley in Italy, Eng. Struct. 49 (2013) 465–490, https://doi.org/10.1016/j.engstruct.2012.11.033.
[21] S. Casolo, Macroscale modelling of the orthotropic shear damage in the dynamics of masonry towers by RBSM, Eng. Fail. Anal. 130 (2021) 105744, https://doi.org/10.1016/j.engfailanal.2021.105744.
[22] A.M. D'Altri, F. Cannizzaro, M. Petracca, D.A. Talledo, Nonlinear modelling of the seismic response of masonry structures: calibration strategies, Bull. Earthq. Eng. 20 (2022) 1999–2043, https://doi.org/10.1007/s10518-021-01104-1.
[23] G. Lacanna, M. Ripepe, M. Coli, R. Genco, E. Marchetti, Full structural dynamic response from ambient vibration of Giotto's bell tower in Firenze (Italy), using modal analysis and seismic interferometry, NDT E Int. 102 (2019) 9–15, https://doi.org/10.1016/j.ndteint.2018.11.002.
[24] G. Standoli, E. Giordano, G. Milani, F. Clementi, Model updating of historical belfries based on OMA identification techniques, Int. J. Architect. Herit. 15 (1) (2021) 132–156, https://doi.org/10.1080/15583058.2020.1723735.
[25] G. Milani, F. Clementi, Advanced seismic assessment of four masonry bell towers in Italy after operational modal analysis (OMA) identification, Int. J. Architect. Herit. 15 (1) (2021) 157–186, https://doi.org/10.1080/15583058.2019.1697768.
[26] A. Ferrante, D. Loverdos, F. Clementi, G. Milani, A. Formisano, S. Lenci, V. Sarhosis, Discontinuous approaches for nonlinear dynamic analyses of an

ancient masonry tower, Eng. Struct. 230 (2021) 111626, https://doi.org/10.1016/j.engstruct.2020.111626.
[27] E. Bertolesi, G. Milani, S. Casolo, Homogenization towards a mechanistic rigid body and spring model (HRBSM) for the non-linear dynamic analysis of 3D masonry structures, Meccanica 53 (7) (2018) 1819–1855, https://doi.org/10.1007/s11012-017-0665-6.
[28] S. Casolo, Macroscopic modelling of structured materials: relationship between orthotropic Cosserat continuum and rigid elements, Int. J. Solid Struct. 43 (3-4) (2006) 475–496, https://doi.org/10.1016/j.ijsolstr.2005.03.037.
[29] J.L. Beck, L.S. Katafygiotis, Updating models and their uncertainties. I: bayesian statistical framework, J. Eng. Mech. 124 (4) (1998) 455–461, https://doi.org/10.1061/(ASCE)0733-9399(1998)124:4(45.
[30] J.L. Beck, S. Au, M.W. Vanik, Monitoring structural health using a probabilistic measure, Comput. Aided Civ. Infrastruct. Eng. 16 (1) (2001) 11, https://doi.org/10.1111/0885-9507.00209.
[31] R. Rocchetta, M. Broggi, Q. Huchet, E. Patelli, On-line Bayesian model updating for structural health monitoring, Mech. Syst. Signal Process. 103 (2018) 174–195, https://doi.org/10.1016/j.ymssp.2017.10.015.
[32] C. Pepi, M. Gioffrè, M.D. Grigoriu, Bayesian inference for parameters estimation using experimental data, Probab. Eng. Mech. 60 (2020) 103025, https://doi.org/10.1016/j.probengmech.2020.103025.
[33] A. Murano, J. Ortega, H. Rodrigues, G. Vasconcelos, Updating mechanical properties of two-leaf stone masonry walls through experimental data and Bayesian inference, Constr. Build. Mater. 298 (2021) 123626, https://doi.org/10.1016/j.conbuildmat.2021.123626.
[34] L. Ierimonti, N. Cavalagli, I. Venanzi, E. Garcìa-Macìas, F. Ubertini, A transfer Bayesian learning methodology for structural health monitoring of monumental structures, Eng. Struct. 247 (2021) 113089, https://doi.org/10.1016/j.engstruct.2021.113089.
[35] S. Monchetti, C. Pepi, C. Viscardi, M. Gioffrè, Approximate bayesian computation for structural identification of ancient tie-rods using noisy modal data, Probab. Eng. Mech. 77 (2024) 103674, https://doi.org/10.1016/j.probengmech.2024.103674.
[36] M.C. Kennedy, A. O'Hagan, Bayesian calibration of computer models, J. Roy. Stat. Soc. B Stat. Methodol. 63 (3) (2001) 425–465, https://doi.org/10.1111/1467-9868.00294.
[37] P.D. Arendt, D.W. Apley, W. Chen, Quantification of model uncertainty: calibration, model discrepancy, and identifiability, J. Mech. Des. 134 (10) (2012) 100908, https://doi.org/10.1115/1.4007390.
[38] J. Brynjarsdóttir, A. O'Hagan, Learning about physical parameters: the importance of model discrepancy, Inverse Probl. 30 (11) (2014) 114007, https://doi.org/10.1088/0266-5611/30/11/114007.
[39] G.E.P. Box, G.C. Tiao, Bayesian Inference in Statistical Analysis, Wiley, NY, 1992. ISBN: 978-0-471-57428-6.
[40] S.H. Cheung, J.L. Beck, Bayesian model updating using hybrid monte carlo simulation with application to structural dynamic models with many uncertain parameters, J. Eng. Mech. 135 (4) (2009) 243–255, https://doi.org/10.1061/(ASCE)0733-9399(2009)135:4(243.
[41] B. Goller, G.I. Schuëller, Investigation of model uncertainties in Bayesian structural model updating, J. Sound Vib. 330 (25) (2011) 6122–6136, https://doi.org/10.1016/j.jsv.2011.07.036.
[42] CNR, CNR-DT 212/2013 – Guide for the Probabilistic Assessment of the Seismic Safety of Existing Buildings, Consiglio Nazionale delle Ricerche, Roma, 2013. https://www.cnr.it/en/node/2643.
[43] P. Spinelli, L. Salvatori, R. Lancellotta, M. Betti, Preliminary assessment of the seismic behaviour of Giotto's bell tower in florence, Int. J. Architect. Herit. 17 (1) (2023) 23–45, https://doi.org/10.1080/15583058.2022.2145527.
[44] S. Casolo, A three-dimensional model for vulnerability analysis of slender medieval masonry towers, J. Earthq. Eng. 2 (4) (1998) 487–512, https://doi.org/10.1080/13632469809350332.
[45] E. Simoen, G. De Roeck, G. Lombaert, Dealing with uncertainty in model updating for damage assessment: a review, Mech. Syst. Signal Process. 56–57 (2015) 123–149, https://doi.org/10.1016/j.ymssp.2014.11.001.
[46] K. Yuen, Bayesian Methods for Structural Dynamics and Civil Engineering, John Wiley & Sons, 2010. ISBN:9780470824542.
[47] I. Behmanesh, B. Moaveni, C. Papadimitriou, Probabilistic damage identification of a designed 9-story building using modal data in the presence of modeling errors, Eng. Struct. 131 (2017) 542–552, https://doi.org/10.1016/j.engstruct.2016.10.033.
[48] M. Tomaževič, M. Lutman, L. Petkovic, Seismic behavior of masonry walls: experimental simulation, ASCE J. Struct. Eng. 122 (9) (1996) 1040–1047, https://doi.org/10.1061/(ASCE)0733-9445(1996)122:9(1040.